Calcination of Octadecasil: Fluoride Removal and Symmetry of the Pure SiO_2 Host

Luis A. Villaescusa, Philip A. Barrett, and Miguel A. Camblor*

Instituto de Tecnología Química, Avda. Los Naranjos s/n, 46071 Valencia, Spain

Received June 8, 1998. Revised Manuscript Received September 11, 1998

Pure silica octadecasil (AST) has been synthesized hydrothermally in a fluoride medium using a new structure-directing agent (*tert*-butyltrimethylammonium). F^- is occluded in the material inside the small [4^6] cage and is removed completely upon calcination, in sharp contradiction with recent predictions based on computational studies. We propose chemically feasible pathways for the migration of F^- out of the [4^6] cage that are based on the known chemical reactivity of F^- and SiO_2 and on the presence of small cations formed by thermal degradation of the organic species. After calcination to remove the guest species, the structural integrity of the host is completely preserved, yielding a pure SiO_2 framework devoid of connectivity defects. Its structure has been solved by direct methods and refined using synchrotron X-ray powder diffraction data. Despite the removal of guest species, the framework is seen to adopt a tetragonal symmetry rather than the cubic maximum topological symmetry. It is proposed that symmetry lowering in AST is a consequence of the energetically unfavorable angles in the higher space group, in which 20% of the Si present four linear Si−O−Si angles. ^{29}Si MAS NMR spectroscopy and energy minimization calculations support this notion and the refined structure proposed. At 500 °C calcined octadecasil undergoes a reversible phase transition to pseudocubic symmetry. Finally, the reported $AlPO_4$-16 or octadecasil cubic forms are proposed to actually be disordered pseudocubic structures.

Introduction

The structures of zeolites and pure silica phases frequently display a symmetry lower than the maximum topological symmetry. This probably reflects the existence of energetically unfavorable configurations within the framework when the maximum symmetry is assumed. However, it is not always straightforward to explain the reasons for the symmetry lowering. The presence of so-called extraframework species or a distribution of different tetrahedral atoms along the framework makes a detailed investigation of the reasons for symmetry lowering difficult in zeolites. An added problem limiting the level of information obtainable in a number of materials, notably clathrasils, is that removal of the guest species cannot be accomplished without significant framework damage.

In the case of octadecasil (structure code AST),[1] the maximum topological symmetry is cubic ($Fm\bar{3}m$) while the as-made form (which occludes around equivalent amounts of F^- anions and protonated quinuclidinium cations) was reported to crystallize in the tetragonal system ($I4/m$).[2] In principle, this could possibly be related to a distortion of the framework due to the presence of the guest species. Unfortunately, calcination of this octadecasil to completely remove the organics was not possible without partial collapse of the structure.[2,3] Thus, the detailed structure of the pure silica framework has never been reported. However, after calcination at 500 °C in air the black product obtained was described as having a cubic structure.[2,3] Moreover, F^- was recently predicted to stay in the material after calcination,[4] and this could certainly affect its structure.

We have now synthesized octadecasil using a different structure-directing agent which can be completely removed along with F^- by calcination. We report here on the structural characterization of the pure SiO_2 phase and discuss in detail its symmetry. Octadecasil has one of the most simple structures among the nondense SiO_2 phases and now can be prepared as an SiO_2 framework devoid of guest species, which makes this material a good reference for structural studies of this important class of silicates.

Experimental Section

Synthesis of *tert*-Butyltrimethylammonium. The organic cation used as the structure-directing agent (SDA) for the synthesis of octadecasil was prepared by methylation of *tert*-butylamine with methyl iodide in chloroform at room temperature. In a typical synthesis, 51.72 g of $K_2CO_3 \cdot 1.5H_2O$ (99%, Aldrich) was added to a solution made by dissolving 25.79 g of *tert*-butylamine (98%, Aldrich) in 294.05 g of $CHCl_3$.

(1) Meier, W. M.; Olson, D. H.; Baerlocher, Ch. *Atlas of Zeolite Structure Types*, 4th ed.; Elsevier: Amsterdam, 1996.
(2) Caullet, P.; Guth, J. L.; Hazm, J.; Lamblin, J. M.; Gies, H. *Eur. J. Solid State Inorg. Chem.* **1991**, *28*, 345.
(3) Kessler, H.; Patarin, J.; Schott-Darie, C. In *Advanced Zeolite Science and Applications*; Jansen, J. C., Stöcker, M., Karge, H. G., Weitkamp, J., Eds.; Elsevier: New York, 1994; p 75.
(4) George, A. R.; Catlow, C. R. A. *Zeolites* **1997**, *18*, 67.

10.1021/cm9804113 CCC: $15.00
Published on Web 11/04/1998

The resulting mixture was immersed in an ice bath and then around 27 mL of CH_3I was added dropwise under stirring. After 1 week of continuous stirring at room temperature, the mixture was filtered and the *tert*-butyltrimethylammonium iodide was extracted from the solid in a Soxhlet using CH_2Cl_2 as the solvent. After evaporation of the solvent, 75.44 g (88% yield) of a white solid was obtained. Chemical analysis found 5.87 N, 34.65 C, 7.50 H. Expected for $C_7H_{18}NI$: 5.76 N, 34.58 C, 7.46 H.

The SDA was anion exchanged to the hydroxide form by contacting overnight a solution of the iodide with a strongly basic Dowex anion-exchange resin under stirring. After filtering, washing, and concentrating under vacuum, a solution of $C_7H_{18}NOH$ was obtained and titrated with 0.1 N HCl using phenolphthalein. Typically, the yield of the anion exchange was around 95%.

Synthesis of Octadecasil. The synthesis was performed hydrothermally using F^- as a mineralizer and *tert*-butyltrimethylammonium as SDA. In a typical synthesis, 20.44 g of tetraethylorthosilicate (98%, Merck) was hydrolyzed in 33.97 g of an aqueous solution of the SDA in hydroxide form ($1.44 \cdot 10^{-3}$ mol of OH^-/g of solution). The mixture was stirred to allow complete evaporation of the ethanol produced (plus some water). A weight loss of 23.51 g was produced in the process. Then, 2.04 g of HF (48%, Merck) was added with stirring. The thick paste obtained was homogenized by hand stirring. The mixture was then transferred to Teflon-lined stainless steel 60 mL autoclaves which were rotated at 60 rpm while being heated at 150 °C for 6 days. The products (pH = 8.3) were filtered and the solids washed and dried overnight at 100 °C. A yield of 19.8 g of solid per 100 g of reacting mixture was obtained.

Characterization. Phase purity and crystallinity were determined by conventional powder X-ray diffraction (XRD) using a Philips X'Pert diffractometer (Cu Kα radiation, graphite monochromator) provided with a variable divergence slit and a proportional Xe detector and working in the fixed irradiated area mode. In situ XRD measurements at high temperature under ambient air were recorded on the same apparatus using an Anton Parr HTK 16 camera provided with a 1 mm thick Pt filament and a DL 540 position-sensitive detector (PSD) from Raytech, recording statically in the range 21−31° 2θ. C, H, and N contents were determined with a Carlo Erba 1106 elemental organic analyzer. Fluoride content was determined using an ion-selective electrode connected to a Mettler Toledo 355 ion analyzer after dissolution of the as-made solids by a standard procedure.[5] Thermogravimetric analyses were performed on a NETZSCH STA 409 EP thermal analyzer in the 293−1173 K range with ca. 0.0200 g of sample, a heating rate of 10 K/min, and an air flow of 6 L/h. ^{29}Si, ^{1}H, and ^{13}C MAS NMR spectra of the solids were recorded on a Varian VXR 400SWB spectrometer. The ^{29}Si MAS NMR spectra was recorded with a spinning rate of 5.5 kHz at a ^{29}Si frequency of 79.459 MHz with a 55.4° pulse length of 4.0 μs and a recycle delay of 80 and 240 s. The ^{13}C MAS NMR spectrum was acquired with a spinning rate of 5.1 kHz at a ^{13}C frequency of 100.577 MHz with a 24° pulse length of 2.0 μs and a recycle delay of 60 s. The ^{1}H MAS NMR spectrum was recorded with a spinning rate of 7.0 kHz at a ^{1}H frequency of 399.956 MHz with a pulse length of 1.0 μs and a recycle delay of 5.0 s. All ^{1}H, ^{29}Si, and ^{13}C chemical shifts are reported relative to TMS. The ^{19}F MAS NMR spectrum was recorded in a Varian 300 spectrometer at a spinning speed of 7 kHz, at a frequency of 282.187 MHz with a 38.6° pulse length of 3 μs and a recycle delay of 5s. The ^{19}F chemical shift was referenced to $CFCl_3$. The infrared spectrum in the region of framework vibrations (300−1900 cm^{-1}) was recorded in a Nicolet 710 FTIR spectrometer using the KBr pellet technique.

Synchrotron X-ray Data Collection and Structure Analysis. Synchrotron X-ray powder diffraction data were collected on calcined octadecasil on station 2.3 of the Daresbury SRS in flat plate mode using the parameters summarized in Table 1. Inspection of both the high-resolution data as well as conventional laboratory XRD data clearly confirmed that the tetragonal symmetry proposed by Caullet et al.[2] for the templated solid is maintained after calcination. The high crystallinity of the material following calcination permitted the solution of the structure from laboratory X-ray data by direct methods in the program Sirpow[6] from Le Bail[7] intensities extracted using the Mprofil program suite.[8] Synchrotron data though was preferred for the structure refinement due to the superior resolution and peak shape. The unit cell parameters for the calcined octadecasil were first refined in the program REFCEL[9] before Rietveld refinement[10] was undertaken using the GSAS suite of programs.[11] A pseudo-Voigt function[12] was used to describe the peak shape together with a manually interpolated background. A model for the framework atoms in space group *I*4/*m* was taken from the direct methods results using laboratory X-ray data. In the initial stages the scale factor, peak shape, unit cell parameters, and zero point were refined first before the atomic positional parameters were allowed into the refinement. The thermal parameters were treated isotropically and refined together with the atomic positions and nonstructural parameters in the final stages of the refinement. The model quickly converged to the residuals[11] $R_p = 7.72$, $R_{wp} = 9.87$, and $R_b = 3.91$, for which no constraints were used.

Energy minimization calculations were subsequently applied to examine the energetics of the calcined structure in comparison to the cubic symmetry proposed in other studies[13,14] and observed to exist in this material upon high-temperature treatment (see below). In all the calculations attempted, the GULP code[15] was used together with the silicate potentials of Saunders et al.,[16] which include a shell model[17] description of ionic polarization and the rational function optimization (RFO) algorithm,[18] to ensure that the correct minima were located.

Table 1. Data Collection and Crystallographic Parameters for Calcined Octadecasil

wavelength	1.200511 Å
2θ range	6−80°
step size	0.01°
count time	2 s/p
number of data points	6620
number of reflections	382
profile range used (2θ)	10−80°
number of profile parameters	9
number of structural parameters	16
number of constraints	0
unit cell	a = 9.25505(15) c = 13.50068(25)
space group	*I*4/*m* (87)
residuals	$R_{exp} = 5.26$ $R_p = 7.72$ $R_{wp} = 9.87$ $R_b = 3.91$

(5) Guth, J. L.; Wey, R. *Bull. Soc. Fr. Minéral. Cristallogr.* **1969**, *92*, 105.

(6) Atomare, A.; Burla, C.; Cascarano, C.; Cascarino, C.; Giacovazzo, C.; Gualiardi, A.; Polidori, G.; Canalli, R. M. *J. Appl. Crystallogr.* **1994**, *27*, 435.

(7) Le Bail, A. *Mater. Res. Bull.* **1988**, *23*, 447.

(8) Murray, A. D.; Fitch, A. N. Mprofil program for Le Bail decomposition and profil refinement, 1990.

(9) Refcel program for unit cell refinement, Daresbury Laboratory.

(10) Rietveld, H. M. *J. Appl. Crystallogr.* **1969**, *2*, 65.

(11) Larson, A.; Von Dreele, R. B. GSAS Manual, Los Alamos Report No. LA-UR-86-748, 1986.

(12) Hastings, J. B.; Thomlinson, W.; Cox, D. E. *J. Appl. Crystallogr.* **1984**, *17*, 85

(13) Bennett, J. M.; Kirchner, R. M. *Zeolites* **1991**, *11*, 502.

(14) Schreyeck, L.; Caullet, P.; Mougenel, J. C.; Patarin, J.; Paillaud, J. L. *Microporous Mater.* **1997**, *11*, 161.

(15) Gale, J. D. *J. Chem. Soc., Faraday Trans.* **1997**, *93*, 629

(16) Saunders, M. J.; Leslie, M.; Catlow, C. R. A. *J. Chem. Soc. Chem. Commun.* **1984**, 1273.

(17) Dick, B. G.; Overhauser, A. W. *Phys. Rev.* **1958**, *112*, 90.

(18) Simons, J.; Jørgensen, P.; Taylor, H.; Oyment, J. *J. Phys. Chem.* **1983**, *87*, 2745

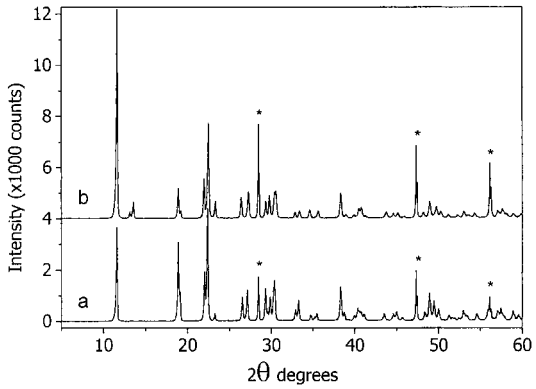

Figure 1. Powder XRD patterns of as-made (a) and calcined (b) silica octadecasil. Peaks marked with an asterisk correspond to Si (internal standard).

Table 2. Chemical Composition

N (wt %)	C (wt %)	H (wt %)	F (wt %)	C/N	F/N
1.92	11.64	2.46	2.39	7.06	0.92

Results and Discussion

The use of *tert*-butyltrimethylammonium in fluoride medium allowed the synthesis of octadecasil as a highly crystalline phase. Its XRD pattern (Figure 1a) was indexed as tetragonal with $a = 9.30$ Å and $c = 13.45$ Å and with systematic absences consistent with a body-centered symmetry. Chemical analysis (Table 2) suggests the organic SDA is occluded intact within the framework and its charge is mainly balanced by occluded F^-. A small charge misbalance suggests a minor presence of connectivity defects in the as-made material. From chemical analysis and based on both the previously proposed structure for quinuclidinium octadecasil and the need for connectivity defects, a plausible chemical formula for the unit cell is $[C_7H_{18}NF_{0.92}]_2[Si_{20}O_{40}(OH)_{0.16}]$. The organic cations, due to their large size, must be located in the large $[4^66^{12}]$ cages, while the F^- anions have been located by single-crystal X-ray diffraction in the small $[4^6]$ cage in the as-made octadecasil synthesized with quinuclidinium.[2] A single, narrow resonance at −38.5 ppm in the ^{19}F MAS NMR spectrum of our sample (not shown) and at −38.2 ppm in the previous report[2] suggests F^- is also located in the $[4^6]$ cage in our material.

^{13}C MAS NMR spectroscopy (not shown) also supports the conclusion that the SDA is occluded intact within the framework, as there are only three resonances at 71.9 (tertiary carbon), 50.0 (methyl groups bonded to charged N), and 24.4 ppm (methyl groups in the *tert*-butyl moiety). These chemical shifts are very close to those in the ^{13}C NMR spectrum of *tert*-butyltrimethylammonium iodide in D_2O solution (71.3, 49.1, and 23.1 ppm, respectively). The ^1H MAS NMR spectrum (Figure 2) contains two lines of roughly equal intensity at 3.2 (methyl groups bonded to charged N) and 1.6 ppm (methyl groups in the *tert*-butyl moiety), in agreement with the chemical shifts of *tert*-butyltrimethylammonium in D_2O (3.0 and 1.5 ppm). This further supports the integrity of the occluded SDA. There are also two small bands at 5.7 and 4.6 ppm. Their chemical shifts are near the range previously found for water molecules associated with alkali-metal cations in high-silica zeolites.[19] However, due to the lack of alkali cations in our material, these bands should be assigned to Si−OH groups forming relatively weak hydrogen bonds, possibly including silanols in the outer surface of the crystallites. The band at 4.6 ppm could also be due to small water clusters inside the clathrasil or to moisture in its outer surface (^1H in liquid water resonate at about 4.8 ppm). These bands amount altogether to 1 H/unit cell, as calculated from the estimated ratio of their intensity to the total intensity of organic protons. Finally, there is also a broad line at 9.8 ppm which is visible only when the ^1H MAS NMR spectrum is greatly expanded. Following the arguments in ref 19, this most likely arises from protons in silanol groups forming rather strong Si−O−H···$^-$O−Si hydrogen bonds. These hydrogen bonds are somewhat weaker than usually found in high-silica zeolites synthesized in OH^- media, where the band consistently appears at around 10.2 ppm.[19] The 9.8 ppm resonance is, however, very weak and the concentration of such protons is less than 0.03 per unit cell.

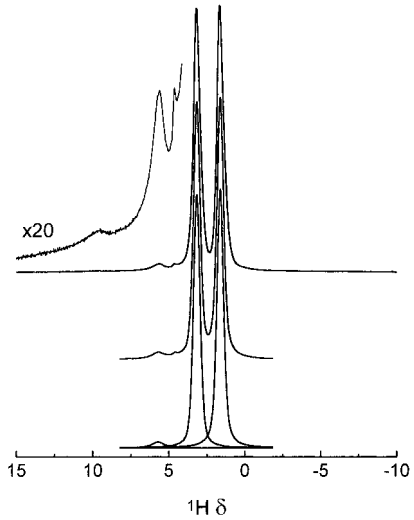

Figure 2. ^1H MAS NMR spectrum of as-made octadecasil (upper traces), with the deconvoluted components and simulated spectra (lower traces).

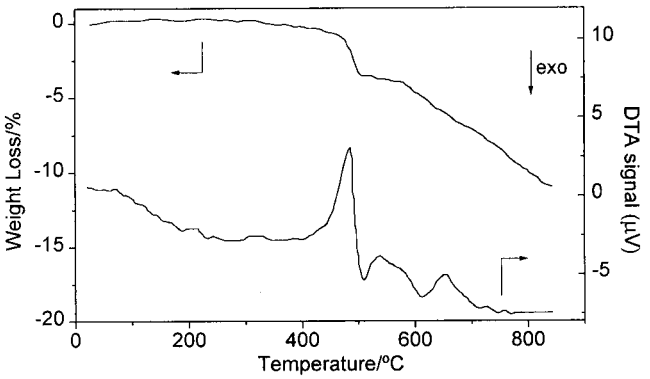

Figure 3. Thermogravimetric (top) and differential thermal analysis (bottom) traces of as-made octadecasil.

Thermal analysis of the as-made material in flowing air shows several steps of weight loss, all occurring at rather high temperatures (Figure 3). The first weight loss at around 490 °C is associated with an endothermic process followed by a partially overlapping exothermic

(19) Koller, H.; Lobo, R. F.; Burkett, S. L.; Davis, M. E. *J. Phys. Chem.* **1995**, *99*, 12588.

peak. Then, a continuous weight loss associated mainly with exothermic processes occurs at higher temperatures. The most interesting process is obviously the first one, because an endothermic peak at 490 °C due to organic removal is unusual in the heating of zeolites in air, where exothermic burning is typically detected in this range of temperatures. Thus, before combustion of the organic encapsulated in octadecasil, there is an endothermic thermal decomposition which possibly may occur through an E_1 elimination reaction with formation of a stable tertiary carbocation followed by proton transfer to yield isobutene and trimethylammonium. This could afford removal of HF with proton transfer from the trialkylammonium (a proposed mechanism for the removal is discussed below), explaining the ca. 3% weight loss associated with this process (Figure 3). This loss is in rough agreement with the amount of fluoride in the material (Table 2). Evolved HF could not be detected by mass spectrometry, most probably due to the reaction of HF with the ceramics of the oven or with the gas transfer line, which is made of silica. We then designed the following experiment trying to trap evolved HF by reaction with $Ca(OH_2)$: octadecasil and $Ca(OH)_2$ were thoroughly mixed, pelletized, and calcined up to 550 °C. At this temperature the endothermic process is already completed and no other weight loss has started (Figure 3). After calcination, the unreacted $Ca(OH)_2$ was removed by washing with diluted HCl several times, and the resulting solid was shown by XRD to be a mixture of octadecasil and around 5% CaF_2 (determined by peak area). This amount agrees with the F content of as-made octadecasil (Table 2), suggesting HF is removed before 550 °C and supporting the above interpretation of the 490 °C endothermic peak and weight loss.

Calcination at 950 °C in air for 3 h of an as-made octadecasil with a crystallite size <0.25 μm allows complete removal of the organic and fluoride guests and yields a white product without structural damage. Some syntheses under slightly different conditions yielded bigger crystallites (around 0.5−1 μm). In these cases it proved necessary to repeat the calcination four times before a white product was obtained. However, the crystallinity of the material was preserved, showing the very high thermal stability of this SiO_2 phase. The XRD pattern (Figure 1b) evidences the tetragonal body-centered symmetry of the calcined material. This rules out the possibility that symmetry lowering with respect to the maximum topological symmetry of AST was exclusively due to the presence of the occluded organic or fluoride ions. The unit cell was indexed as body-centered tetragonal with a = 9.26 Å, c = 13.51 Å, indicating that there is a small unit cell contraction of around 0.4% upon calcination.

Only traces of F could be detected in the calcined material (≤0.14 wt % compared to 2.4% before calcination), contrary to recently published calculations which concluded that the high activation energy calculated for the migration of F^- out of the [4^6] cage "probably excludes the possibility of extracting the F^- anion from the D4R of octadecasil" and results in its "retention in the structure after calcination".[4] Experimentally this is not the case, and the wrong prediction and conclusion in ref 4 is most likely a consequence of neglecting the

Scheme 1

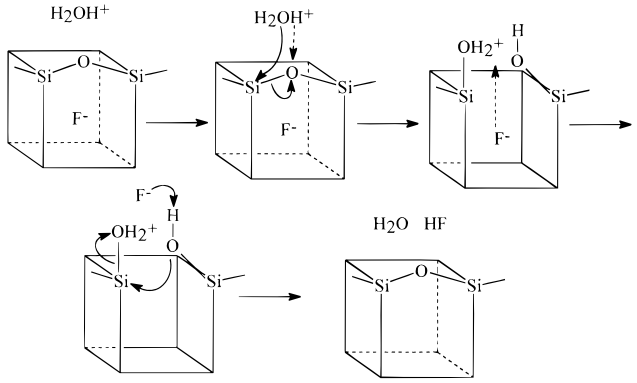

Scheme 2

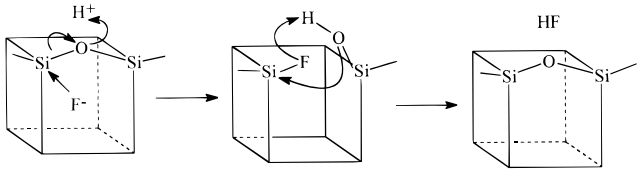

chemical reactivity of F^- and SiO_2 as well as the presence of the organic countercation and its probable degradation products.

With respect to the organic cation we have to consider that, on one hand, the electric charge must be conserved during the decomposition of organic alkylammonium cations. Whereas, on the other hand, the small size of the 6MR windows of the AST structure limits the diffusion of the degraded products out of the material. This makes highly plausible the formation of smaller charged fragments (such as R_3NH^+, $R_2NH_2^+$, RNH_3^+, and finally NH_4^+ and/or H^+; see above). These species are all Brønsted acids and thus may be predicted to effectively catalyze the breaking and closure of Si−O−Si bonds within the silica structure by hydrolysis (with ambient moisture or H_2O formed upon burning of alkyl groups) or amonolysis (with NH_3 coming from the degradation of the organic cation); Scheme 1 depicts an idealized reaction path for the hydrolysis case.

Another very plausible chemical pathway for the migration of F^- out of the [4^6] cage is a nucleophilic attack of F^- onto one Si in the cage, affording the breaking of the siloxy bridge, as shown in Scheme 2.

Although we cannot exclude a mechanism based on Scheme 1, we prefer the one in Scheme 2 in view of its simplicity and the experimental evidence for the existence of the type of interactions involved. As a matter of fact, a critical requirement in this pathway is the first nucleophilic attack of F^- in the presence of a small cation able to polarize one oxygen bridge strongly enough to allow the opening of the bridge. The nucleophilic attack involves a strong interaction between F^- and a Si atom tetrahedrally bonded to four oxygens. Very recent ^{29}Si MAS NMR results[20,21] strongly support the existence of such interactions in zeolites synthesized in the fluoride medium in situations that range from direct Si−F bonding (as in nonasil, with a Si−F distance

(20) Koller, H.; Wölker, A.; Eckert, H.; Panz, C.; Behrens, P. *Angew. Chem. Int. Ed. Engl.* **1997**, *36*, 2823.

(21) Koller, H.; Wölker, A.; Valencia, S.; Villaescusa, L. A.; Díaz-Cabañas, M. J.; Camblor, M. A. Manuscript in preparation.

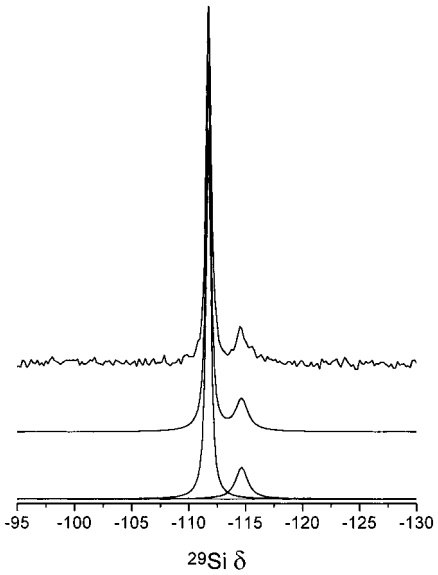

Figure 4. ^{29}Si MAS NMR spectrum of calcined SiO_2 octadecasil: experimental (top), simulation (middle), and deconvoluted components (bottom).

of 1.84 Å) to dynamic situations with F jumping between different Si sites.

Both possibilities (Si−O−Si breaking through either hydrolysis or nucleophilic attack by F^-) make feasible the migration of F^- out of the [4^6] cage. Graphically, ref 4 only considers F^- as leaving directly through a 4MR window, whereas the crucial difference in Scheme 2 is that F^- actually "opens" the window to go out (and "closes" it afterward). In retrospect, it is somewhat unfortunate that F^- leaves the cage, since if it were able to remain, a very interesting new kind of acid material could have resulted.

In the ^{29}Si MAS NMR spectrum of the calcined material (Figure 4), no line in the −95 to −105 ppm region attributable to Si−OH defect groups is detected. Thus, the small concentration of defect groups concluded from the charge unbalance in the as-made material (see above) is apparently healed upon calcination. There are only two resonances at −111.7 and −114.6 ppm which correspond to $Si(OSi)_4$ groups in different crystallographic sites. The intensity ratio of these lines is 4.4:1, which is close but slightly larger than the Si1:Si2 occupancy ratio (4; see below). This small deviation from the expected value is probably due to a significantly longer relaxation time for Si2, as suggested by an increase in the intensity ratio from 4.4 to 6.4 as the recycle delay decreases from 240 to 80 s. The expected chemical shifts of both $Si(OSi)_4$ resonances calculated by applying the equation of Thomas et al.[22] to the mean Si−O−Si angles obtained by Rietveld refinement for each crystallographic site (see below) are in very good agreement (−111.3 and −113.3 ppm for Si1 and Si2, respectively) with the experimental values. We note that the maximum topological symmetry for AST (space group $Fm\bar{3}m$) requires site Si2 to have four linear Si−O−Si angles, so its expected chemical shift (near −130 ppm) would compare unfavorably with the experimental value (−114.6 ppm).

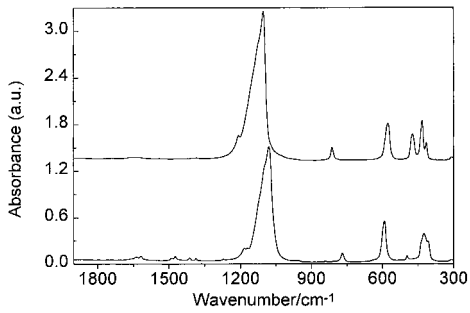

Figure 5. Infrared spectra of as-made (bottom) and calcined (top) silica octadecasil.

Table 3. Atomic Positions for Calcined Octadecasil with Esd's in Parenthesis

atom	*x*	*y*	*z*	U_{iso}
Si(1)	0.23297(17)	0.03657(17)	0.38625(10)	0.024(3)
Si(2)	0.5	0	0.25	0.0181(9)
O(3)	0.16338(32)	0.88142(31)	0.36278(18)	0.0291(10)
O(4)	0.37264(29)	0.05998(28)	0.31732(16)	0.0105(8)
O(5)	0.28242(42)	0.04312(50)	0.5	0.0280(14)

The infrared spectra of as-made and calcined octadecasil are shown in Figure 5. In addition to the disappearance of bands assignable to the organic cation, the region below 800 cm^{-1} changes substantially upon calcination, giving narrower and better resolved lines in the pure silica calcined sample. We note here that changes upon calcination in the infrared spectrum of zeolites synthesized in OH^- medium are generally not as noticeable as those observed in Figure 5. This region has been classically assigned to small structural subunits, perhaps because it is the region showing more specific features of each zeolitic structure. However, it is unclear and still controversial as to whether[23] or not[24] it is possible to assign vibrational bands to localized vibrations of specific subunits in zeolites. Whatever the assignment, the changes upon calcination observed in Figure 5 suggest that the presence of F^- in the small interstices of the framework, possibly interacting strongly with framework Si,[21] produces distortions in the (either extended or localized) vibrational modes that disappear after calcination, as already observed for pure silica zeolite β[25] and ITQ-4.[26]

Structure Analysis. Final atomic coordinates and distances and angles for calcined octadecasil, derived from Rietveld refinement, are given in Tables 3 and 4, respectively, and the Rietveld plot is presented in Figure 6. The full pattern Rietveld refinement results clearly show the structure to be intact and that none of the guest species, the template entrapped in the truncated rhombododecahedral cages, and the F^- counterions proposed to reside within the double four ring units within the structure[2,13,14] are still present after calcination. The average Si−O distances (Si(1) = 1.607 Å and Si(2) = 1.589 Å) and average O−Si−O angles (Si(1) = 109.45° and Si(2) = 109.47°) are very close to the ideal tetrahedral geometry expected, within space group *I*4/*m* all the Si−O−Si angles (average = 148.50°) also being in good agreement with those typically cited for this class

(22) Thomas, J. M.; Klinowski, J.; Ramdas, S.; Hunter, B. K.; Tennakoon, D. T. B. *Chem. Phys. Lett.* **1983**, *102*, 158.

(23) Iyer, K. A.; Singer, S. J. *J. Phys. Chem.* **1994**, *98*, 12670

(24) de Man, A. J. M.; van Santen, R. A. *Zeolites* **1992**, *12*, 269.

(25) Camblor, M. A.; Corma, A.; Valencia, S. *J. Mater. Chem.* **1998**, *8*, 2137.

(26) Barrett, P. A.; Camblor, M. A.; Corma, A.; Jones, R. H.; Villaescusa, L. A. *J. Phys. Chem.* **1998**, *102*, 4147.

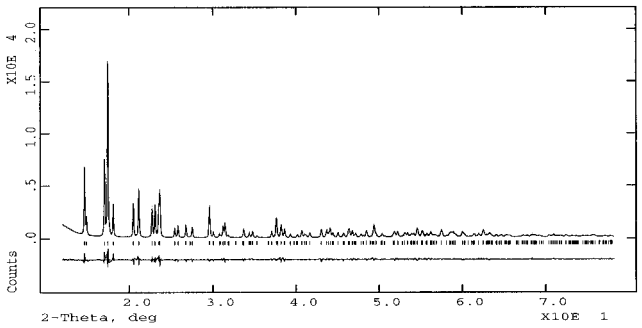

Figure 6. Observed (dots) and calculated (solid line) X-ray diffraction patterns for calcined pure silica octadecasil (wavelength 1.200511 Å) following Rietveld refinement. Vertical ticks indicate the positions of allowed reflections in space group *I*4/*m*. The lower trace is the difference plot.

Table 4. Framework Bond Distances and Angles for Calcined Octadecasil

bond	(Å)	angle	(deg)
Si(1)−O(3)	1.6053(28)	O(3)−Si(1)−O(3)	110.42(24)
Si(1)−O(3)	1.6120(28)	O(3)−Si(1)−O(4)	109.20(18)
Si(1)−O(4)	1.6075(25)	O(3)−Si(1)−O(5)	109.71(22)
Si(1)−O(5)	1.6035(17)	O(3)−Si(1)−O(4)	108.43(17)
		O(3)−Si(1)−O(5)	110.37(21)
		O(4)−Si(1)−O(5)	108.66(18)
Si(2)−O(4)	1.5886(24)	O(4)−Si(2)−O(4)	110.20(17)
Si(2)−O(4)	1.5886(24)	O(4)−Si(2)−O(4)	109.11(8)
Si(2)−O(4)	1.5886(24)	O(4)−Si(2)−O(4)	109.11(8)
Si(2)−O(4)	1.5886(24)	O(4)−Si(2)−O(4)	109.11(8)
		O(4)−Si(2)−O(4)	109.11(8)
		O(4)−Si(2)−O(4)	110.20(17)
		Si(1)−O(3)−Si(1)	147.22(24)
		Si(1)−O(4)−Si(2)	151.74(19)
		Si(1)−O(5)−Si(1)	146.54(27)

Table 5. Lattice Energies and Unit Cell Dimensions of Octadecasil from Energy Minimization

crystal system	space group	*E* (eV)	relative Δ*E* (eV)	*a* (Å)	*c* (Å)	*V* (Å^3)
tetragonal	*I*4/*m*	−1285.38	0.00	9.198	13.481	1140.54
cubic	$Fm\bar{3}m$	−1285.16	0.22	13.459	13.459	2438.03
tetragonal	*I*4/*mmm*	−1285.16	0.22	9.517	13.459	1219.03
pseudocubic	*I*4/*m*	−1285.35	0.03	9.346	13.217	1154.47

of materials. In the octadecasil type materials including the corresponding aluminophosphate $AlPO_4$-16,[13] cubic symmetries have been claimed.[2,13,14] However, the presence of Si−O−Si angles of 180° suggests some disorder away from this more idealized (topological) symmetry, for example pseudocubic (a tetragonal unit cell with the *c* crystallographic axis constrained such that $c = a\sqrt{2}$, which would not permit the deviation away from cubic symmetry to be detected by powder XRD data).

The energy minimization calculations performed on this system shed some light on this matter. When the symmetry is assumed to be tetragonal and using the space group *I*4/*m*, which was found most suitable from Rietveld refinement, the structure relaxes to the minimum having the most favorable lattice energy with no linear Si−O−Si angles (see Table 5). In the case of the cubic topological symmetry $Fm\bar{3}m$ and the first tetragonal subgroup of this topological symmetry *I*4/*mmm*, the energies are found to be the same and considerably less favorable than the results obtained with space group *I*4/*m*. In the case of *I*4/*mmm*, it is noteworthy that the minimized structure in this symmetry is found to be pseudocubic with the *c* lattice parameter exactly equal to $a\sqrt{2}$ and the unit cell volume almost exactly half of that obtained when the cubic topological symmetry is

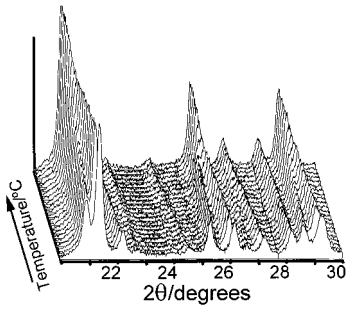

Figure 7. Powder XRD pattern of calcined octadecasil during in situ heating in air. The first trace is the room-temperature pattern. The second one corresponds to 200 °C and the temperature is increased by 20 °C steps for each following pattern up to 600 °C in the last one.

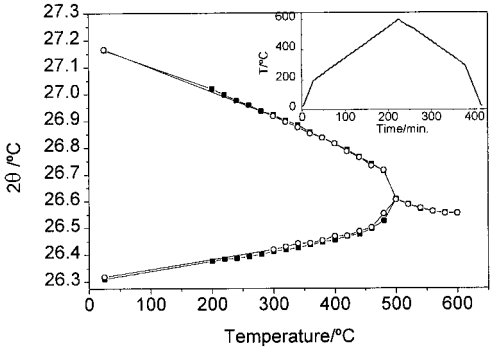

Figure 8. Position of the (220) (top) and (004) (bottom) reflections of tetragonal calcined octadecasil as a function of temperature during in situ heating (■) and cooling (○) in air. At 500 °C both reflections merge in the pseudocubic (400) reflection. The temperature program is shown in the insert.

used. Additionally in these two cases the unit cell obtained is significantly larger than either that found experimentally (V = 1156.42(3) Å^3) or that obtained from the simulations in *I*4/*m*. In both of these two symmetries, however, the less favorable calculated lattice energies can be explained by the presence of symmetry-constrained Si−O−Si angles of 180°.

The XRD patterns of calcined octadecasil recorded at temperatures above 500 °C display a face-centered cubic symmetry (Figure 7). However, upon cooling of the sample below 500 °C, the pattern reverts back to the tetragonal symmetry. This is in contradiction with the behavior reported previously for octadecasil synthesized using quinuclidine, where the calcined material is apparently described as cubic at room temperature.[2] This is probably due to significant structure collapse for those samples[2] or to the presence in them of a high concentration of randomly distributed defects (see below). Calcination of our sample up to 1000 °C did not reveal any loss of crystallinity, and no defects were observed in the ^{29}Si MAS NMR spectrum (see above). Thus, symmetry lowering in octadecasil is not caused simply by the presence of organics or F^- within the SiO_2 host.

The difference in position between the (004) and (220) Bragg reflections can be used as a measure of the tetragonal distortion of octadecasil, as they correspond to the single (400) reflection in the cubic space group $Fm\bar{3}m$. The positions of both reflections as a function of temperature during in situ XRD experiments in air have been plotted in Figure 8. From this figure it

Table 6. Energies and Unit Cell Parameters Results from Free Energy Calculations

	25 °C			550 °C		
	free energy (eV)	*a* (Å)	*c* (Å)	free energy (eV)	*a* (Å)	*c* (Å)
cubic	−1282.86	13.4585		−1286.25	13.5126	
tetragonal	−1283.08	9.2429	13.4415	−1286.76	9.3286	13.4554
pseudocubic	−1283.06	9.3492	13.2217	−1286.78	9.3992	13.2925

becomes apparent that as the temperature increases there is a gradual shift of both reflections, which indicates a decrease in the tetragonal distortion as the thermal motion increases. This suggests that the symmetry change at 500 °C is a result of the averaged symmetry, which becomes pseudocubic as more and more thermal disorder is introduced into the structure. According to this interpretation, the symmetry change at 500 °C would be an orientational order−disorder phase transition. The calculation presented in the last row in Table 5 shows results from a simulation whereby space group *I*4/*m* is assumed to be the ideal symmetry for this structure, and the *c* unit cell axis is constrained to be equal to $a\sqrt{2}$ and hence pseudocubic. The more favorable lattice energies for this system in comparison to those for the cubic and higher tetragonal models suggest this to a be a possible explanation for the changes seen in the diffraction pattern of this material upon heating. The phase transition to cubic symmetry could well be explained by a pseudocubic model which is seen here to be more favorable from the stand point of energy minimization and fit more in line with expectation, since angles of 180° point to disorder which cannot be described by the symmetry in use.

In an attempt to include the effect of temperature in the calculations, since it is only at high temperatures (≥500 °C) that doubts over the true symmetry exist, a set of free energy minimization calculations were attempted using the same potential model and once again employing the GULP code. Two temperatures were studied, 25 and 550 °C, and the free energies obtained together with the unit cell parameters are summarized in Table 6. A clear result from these calculations is that the cubic symmetry is disfavored at both the high and low temperatures, consistent with expectation and with the earlier calculations. The free energies obtained for the tetragonal and pseudocubic symmetries are in both cases similar, though it is interesting that the tetragonal is slightly favored at 25 °C and the pseudocubic at 550 °C (see Table 6). Regarding the unit cell parameters obtained from the calculations, it is pleasing that at 25 °C the cell parameters obtained for the *I*4/*m* model are in reasonable agreement with those found experimentally. Furthermore, the calculations show in all symmetries that the unit cell expands at the higher temperature. However, the volume calculated for the high-temperature cubic phase (2467 Å^3) is much larger than twice the value calculated for the high-temperature tetragonal or pseudocubic phases, 1171 and 1179 Å^3, respectively (compared to a experimental volume at 500 °C of 2 × 1190 ± 10 Å^3). The smaller volume of the tetragonal and pseudocubic phases may be understood considering that the Si2−O−Si1 angles are not linear for these symmetries while they are for the cubic phase. Finally, it is noteworthy that when going from the tetragonal phase at room temperature to the pseudocubic phase at high temperature there is an increase in the *a* cell edge and a decrease in the *c* edge, while an increase in both edges would occur when going from the tetragonal room temperature phase to the high-temperature cubic phase (Table 6). Experimentally we have found that up to 500 °C *a* increases while *c* decreases, as depicted in Figure 8, where the (220) and (004) tetragonal reflections are shown to shift to lower and higher 2θ angles, respectively, during in situ heating. These results further support our conclusion that the high-temperature phase is pseudocubic and that the transition is caused by thermal disorder.

Similarly, we postulate that the previously reported cubic calcined octadecasils, for which significant structure degradation was described,[2] may contain a high concentration of randomly distributed Si−OH defect groups and that the associated disorder results in an average pseudocubic symmetry. This is also probably the case for the isostructural as-made $AlPO_4$-16 synthesized with quinuclidine in the OH^- medium, which was described as having an idealized cubic symmetry.[13] Although the protonation state of quinuclidine in this material was not determined, we note that if there were a significant amount of protonated quinuclidine, then the need for charge balance would force Al−OH $^-$O−P connectivity defects to be present and the associated disorder would be the cause of the increase in the observed average symmetry. The fact that this is a realistic assumption is supported by the observation that when quinuclidine is used to prepare $AlPO_4$-16 in the F^- medium, the as-made material is tetragonal.[27] In this case, charge balance is achieved by inclusion of the equivalent amount of F^-, and thus no defects are required.

Interestingly, $AlPO_4$-16 has been synthesized using several structure-directing agents in F^- medium, and the degree of distortion from the ideal cubic symmetry has been related to the F^- occupancy of the D4R.[14] Thus, in cases where nearly no F^- is found to occupy the D4R, a cubic symmetry is observed, while at a half-occupancy the symmetry is tetragonal. Finally, in one case characterized by the full occupancy of the [4^6] cage by F^- (but one which also contains a large cobalticinium cation within the [$4^6 6^{12}$] cage), the structure was described as monoclinic. In addition to a plausible effect of the organic or organometallic structure-directing agent on the symmetry, we postulate that the presence or absence of randomly distributed defects in these as-made materials, which may be correlated with the presence of F^- in the D4R, may well determine the observed symmetry as a consequence of the different degrees of structural disorder. Calcination of all these $AlPO_4$-16 phases causes a large degree of structural collapse and the XRD pattern is described as cubic.[14] Once again, disorder associated with the presence of structural defects is likely responsible for the symmetry change.

(27) Schott-Darie, C.; Patarin, J.; Le Goff, P. Y.; Kessler, H.; Benazzi, E. *Microporous Mater.* **1994**, *3*, 123.

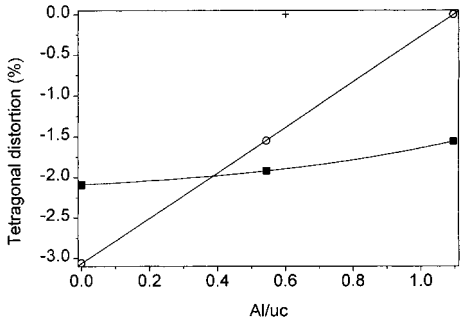

Figure 9. Tetragonal distortion (defined as $(a\sqrt{2} - c)/c$) as a function of the Al content of octadecasil for as-made (■) and calcined (○) samples synthesized in F^- medium and for as-made and calcined samples synthesized in OH^- medium (both represented as a single +). For zero distortion, the powder XRD pattern displays a face-centered cubic symmetry.

To check the above hypothesis concerning the effect of randomly distributed defects on the apparent symmetry of octadecasil, we have tried to synthesized this phase at alkaline pH in the absence of F^-. While we were unable to obtain the pure silica phase, we were successful in the synthesis of a material containing a small amount of Al (around 0.6 Al/unit cell). The amount of negative charges introduced by incorporation of this amount of Al into the framework is not enough to achieve full balance of the occluded cations (2/unit cell), and thus charge balance requires the presence of defects of connectivity. As predicted following the above reasoning, this defect-containing material presented an apparent cubic symmetry in both the as-made and calcined (580 °C) forms, although we were unable to completely remove the organic matter in that sample, which was almost completely destroyed after calcining at 950 °C. By contrast, the material containing the same amount of Al/unit cell obtained in F^- medium presented tetragonal symmetry in both the as-made and calcined forms (Figure 9). On the other hand, when Al is introduced in the framework of octadecasil substituting for Si by direct synthesis in the fluoride medium, the tetragonal distortion of the as-made materials is observed to slightly decrease with the increase in Al content (Figure 9). If, as usual in this kind of materials, isomorphous substitution in tetrahedral positions occurs randomly, the observed decrease in the tetragonal distortion can in turn be explained by the increased degree of disorder as the degree of substitution increases. This effect is most apparent for the calcined aluminosilicates (Figure 9), although in this case a contribution to the disorder by the formation of Si−OH defects if aluminum is extracted from the framework is also possible.

Conclusions

Calcination of a pure silica octadecasil synthesized using *tert*-butyltrimethylammonium in a fluoride medium allows complete removal of both the occluded F^- anions and the organic cations, yielding the pure silica host framework with a high crystallinity and no defects detectable by ^{29}Si MAS NMR. Contrary to previous theoretical predictions, F^- can migrate out of its location in the small [4^6] cages, most likely by opening one of the Si−O−Si edges of the cage. This requires the presence of a small cation by decomposition/burning of the occluded organic cation and can happen by either a hydrolysis reaction or through a nucleophilic attack of F^- onto one of the Si sites in the cage. Clearly, the theoretical prediction failed because a mere physical diffusion of F^- through the 4MR was considered while alternative pathways based on the chemical reactivity of the species involved were neglected.

Calcined SiO_2 octadecasil is tetragonal (space group $I4/m$). The tetragonal symmetry was unexpected, since previous reports on a number of AST materials described them as cubic. We postulate that the symmetry is lowered with respect to the maximum topological symmetry in order to avoid the presence of 20% of the total Si sites having four linear Si−O−Si angles. This energetically unfavorable configuration in the high-symmetry space group is supported by calculations, with an energy penalty of 21 kJ mol^{-1}. Apparently, when an $AlPO_4$-16 or a SiO_2-based AST material presents a high degree of disorder, the symmetry appears as a cubic average from the viewpoint of powder X-ray diffraction. This appears to happen whatever the nature of the disorder: thermal motion, presence of connectivity defects, or large structural damage.

Acknowledgment. The authors greatly acknowledge financial support by the Spanish CICYT (project MAT97-0723). We thank the CLRC for provision of the synchrotron radiation facilities and Dr. C. Tang for assistance with the data collection. P.A.B. is grateful to the European Union TMR program for a postdoctoral fellowship.

CM9804113